Transactions, SMiRT-25
Charlotte, NC, USA, August 4-9, 2019
Division V

ILLUSTRATION OF RITZ VECTOR APPROACH FOR GENERATING IN-CABINET RESPONSE SPECTRA IN CASES OF COMPLEX BOUNDARY CONDITIONS

Pragya Vaishanav[1], Sugandha Singh[1], Abhinav Gupta[2], Sung Gook Cho[3]

[1]Graduate Student, Department of CCEE, North Carolina State University, USA
[2]Director, Center for Nuclear Energy Facilities and Structures, North Carolina State University, USA
[3] CEO, R&D center, Innose Tech Co. LTD, South Korea

INTRODUCTION

Critical safety related equipment are generally mounted on electrical cabinets and must perform well during and after an earthquake. Evaluation of accurate cabinet response is important for seismic qualification of safety equipment. A finite element (FE) analysis or vibration testing for thousands of different cabinets in a nuclear power plant is highly impractical. Ritz vector approach is an efficient and accurate approach for developing the in-cabinet response spectra (ICRS). Mathematically rigorous Ritz vector approach implements method of assumed modes, method of separation, method of superposition and Lagrange's energy methods. It utilizes a set of deformation modes known as Ritz vectors that are consistent with appropriate boundary conditions for cabinet. Often, it is perceived that simplified methods like Ritz vector approach requires idealization of boundary conditions thereby making it impractical for actual applications. In this paper, we present a summary of the Ritz vector approach and use different application examples to illustrate that it can be applied to complex boundary conditions. Its accuracy is evaluated by comparison with the corresponding results from finite element analysis.

Ritz vector approach characterizes the deformation modes of cabinet's plate surfaces or frame members in terms of Ritz vectors. These vectors can be chosen based on appropriate boundary conditions. The number of deformation modes used in the approach can vary depending on the complexity of the boundary conditions. The boundary conditions can sometimes also result in a torsional deformation mode [5, 9] in the structure. Local dissimilarity caused by presence of lumped masses and stiffeners in a plate changes the deformation behavior locally. Rocking at the base of cabinet causes an additional global rigid body mode.

RITZ VECTOR APPROACH

The first step in the Ritz vector approach is to identify the significant modes of deformation for a cabinet's plate or frame member. Dynamic properties of the cabinet can be determined using Raleigh-Ritz method [8] after the shape (Ritz vectors) of these modes are identified based on the boundary conditions. In addition to the local deformation mode of a cabinet's plate or frame, the entire cabinet can exhibit a global deformation mode or a global rocking mode. Displacement u at any location at instant t can be approximately represented by superposition of global and local modes as given in Eq. 1.

$$u(x, y, t) = x_g(t)\phi_g(y) + x_l(t)\phi_l(x, y) \qquad \text{Eq. (1)}$$

where $x_g(t)$ and $x_l(t)$ represent the normal coordinates for global and local modes, respectively as a function of time *t*; $\phi_g(y)$ is the global cabinet mode shape as a function of vertical coordinates y; and $\phi_l(x,y)$ the local mode shape of a plate or frame as a function of horizontal coordinate x and vertical coordinate y. Both $\phi_g(y)$ and $\phi_l(x,y)$ are normalized to unity. The local mode shape $\phi_l(x,y)$ can be further simplified [6] as given in Eq. 2 by applying the method of separation. The local mode shape $\phi_l(x,y)$ of the cabinet still represents a continuous function of coordinates x and y.

$$\phi_l(x,y) = \phi_{lh}(x)\phi_{lv}(y) \qquad \text{Eq. (2)}$$

Sometimes one shape of local component mode is not sufficient to represent the complete deformation. Therefore additional Ritz vectors are added using the method of superposition as shown in Eq. 3.

$$u_l(x,\mathrm{y},t) = \sum_{r=1}^{n} x_r(t)\phi_r(x,\mathrm{y}) \qquad \text{Eq. (3)}$$
$$\phi_r(x,\mathrm{y}) = \phi_{xr}(x)\phi_{yr}(y)$$

Eigen value problem for the generalized system and the corresponding stiffness and mass matrices can be written as,

$$KX = \omega^2 MX$$
$$K = \begin{bmatrix} k_{gg} & k_{gl} \\ k_{lg} & k_{ll} \end{bmatrix};\ M = \begin{bmatrix} m_{gg} & m_{gl} \\ m_{lg} & m_{ll} \end{bmatrix};\ X = \begin{Bmatrix} x_g \\ x_l \end{Bmatrix} \qquad \text{Eq. (4)}$$

where K and M are the stiffness and mass matrices, respectively, and X is the eigenvector. Equation of motion for this cabinet structure can be solved for obtaining the in-cabinet response spectra.

Ritz vector approach utilizes Lagrange's energy method for evaluating the stiffness and mass matrices of the multi degree of freedom system as shown in Eq. 5. The equation differentiates kinetic and potential energy of the structure to derive the mass and stiffness matrices. Various components of the cabinet such as internal frame, the plate, equipment and stiffeners contribute to the total energy of the structure.

$$\frac{\partial T}{\partial \dot{q}} = m\dot{q} \qquad \frac{\partial U}{\partial q} = kq \qquad \text{Eq. (5)}$$

where *T* is the kinetic energy and *U* is the potential energy, q can be either u_l or u_g. Depending upon the term used for q in the equation above, it will give corresponding mass and stiffness term in the matrices. The global cantilever and local component modes contribute to the total kinetic and potential energy (Eq. 6). Plate, horizontal stiffener/frame and vertical stiffener/frame contribute to both the kinetic and potential energy, whereas safety equipment modelled as lumped mass only contributes to the kinetic energy.

$$T = T_g + T_l \qquad U = U_g + U_l$$
$$T_l = T_{lp} + T_{lh} + T_{lv} + T_{lm} \qquad U_l = U_{lp} + U_{lh} + U_{lv} \qquad \text{Eq. (6)}$$

where subscript *g* is the contribution from the global cantilever mode, subscript *l* is the contribution from local component mode, subscript *lp* is for the contribution of plate, subscript *lh* is for the contribution of horizontal stiffener or frame member, *lv* is for the contribution of vertical stiffener or frame member and *lm* is for the contribution of lumped mass.

Usually one or two significant modes are sufficient to represent the complete deformation in plates or frames [2]. Accuracy of dynamic properties calculated in the Ritz vector approach depends on the selection of deformation modes, i.e., Ritz vectors. The selection of Ritz vectors for ϕ_l depends primarily on the boundary conditions and the cabinet properties. Several mathematical functions have been proposed for Ritz vectors by various researchers [1, 2, 3, 6, 11]. Some of the simple and easy-to-use mathematical functions are listed in Table 1. These functions give a mathematical function for the shape of 1-D beam element for the respective boundary conditions at both the ends. In the most simplistic form, one Ritz vector is assumed as the deformation shape along each of the two main axes of the cabinet (*x* & *y*). Cabinets with complex geometry may require superposition of more than one Ritz vector. The participation of additional Ritz vectors often improves the accuracy of the overall approach.

Table 1: Ritz vectors for idealized boundary condition

Description	Mathematical formulation for Ritz vectors
Clamped-Clamped ψ_{cc}	$\cosh\frac{\lambda x}{L} - \cos\frac{\lambda x}{L} - \sigma\left(\sinh\frac{\lambda x}{L} - \sin\frac{\lambda x}{L}\right)$ $\lambda = 4.73004074, \sigma = 0.982502215$
Pinned-Pinned ψ_{pp}	$\sin\frac{\pi x}{L}$
Clamped-Pinned ψ_{cp}	$\cosh\frac{\lambda x}{L} - \cos\frac{\lambda x}{L} - \sigma\left(\sinh\frac{\lambda x}{L} - \sin\frac{\lambda x}{L}\right)$ $\lambda = 3.92660231, \sigma = 1.000777304$
Sliding-Pinned ψ_{sp}	$\cos\frac{\pi x}{2L}$
Clamping-Sliding ψ_{cs}	$\cosh\frac{\lambda x}{L} - \cos\frac{\lambda x}{L} - \sigma\left(\sinh\frac{\lambda x}{L} - \sin\frac{\lambda x}{L}\right)$ $\lambda = 2.36502037, \sigma = 0.982502207$
Free-Free ψ_{ff}	1

APPLICATION EXAMPLES

Simple Plate with Complex Deformation

Most of the cabinets with simple plate geometry require only a single Ritz vector in *x* direction and another Ritz vector in *y* direction. The two Ritz vectors, one in each direction cab be decided based on the boundary condition at the edges of the cabinet. Challenges arise when one Ritz vector is not sufficient to simulate the cabinet. Such is the case when a plate has free boundary condition for two nonadjacent edges and has restraints at other two nonadjacent edges as shown in Figure 1(a).

Left and right edges of this simple plate can move freely. However, due to the restriction on top and bottom edges, the center of the plate experiences restriction away from the edges. Therefore, the deformation of the plate is less in the center and greater near the free edges of the plate, resulting in a concave shape in the *x* direction. A finite element analysis using *SAP2000* can be used to illustrate this shape, as shown in Figure 1(b). The deformation contour of the plate in the figure shows maximum deformation near both the edges, which then reduces near the center of the plate. The side view of the plate in *y* direction also shows the concave shaped deformation at the center.

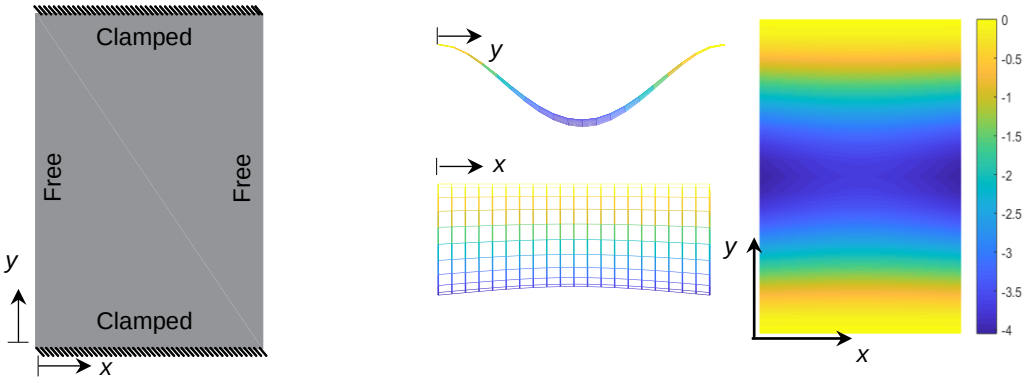

(a) (b)

Figure 1. (a) Simple plate geometry & (b) the deformation contour of the plate obtained from finite element analysis

The challenging part in this case is the non-availability of a standard Ritz vector representing a concave deformation shape. The difficulty in this problem is overcome by using the symmetry in the deformation of the plate in the *x* direction. The half plate can be simulated with one additional Ritz vector (sliding-free) in the *x* direction. The mode shape in *y* direction remains the same as clamped-clamped for both the local modes. The Ritz vector approach will be applied to the half plate and the response is mirrored to find the response of the other half plate. Eq. (7) shows the two Ritz vectors used for the simulation of deformation in this plate using the Ritz vector approach. The good comparison between the ICRS obtained from finite element analysis and Ritz vector approach for the simple plate illustrates the accuracy of this approach (Figure 2). Acceleration record from the El-Centro earthquake is used to develop the ICRS throughout this paper.

$$\phi_{l1}(x,\mathrm{y}) = \psi_{ffx}(x)\psi_{ccy}(y)$$
$$\phi_{l2}(x,\mathrm{y}) = \psi_{sfx}(x)\psi_{ccy}(y) \qquad \text{Eq. (7)}$$

where $\psi_{ffx}(x)$ and $\psi_{sfx}(x)$ represent the free-free and sliding-free boundary condition in the *x* direction for the half plate and $\psi_{ccy}(y)$ represent clamped-clamped boundary condition in the *y* direction

Stiffened Plate with Complex Deformation Shape

Often, cabinets have stiffeners attached to the plate in addition to the simple plate geometry. The stiffeners are attached for strengthening of the plate capacity or to mount the safety equipment. The addition of a stiffener to the plate changes the bending deformation locally or globally. In such cases, the deformation or bending of the plate I is governed by the boundary conditions at the edges of plate and as well as the location

and properties of the stiffener. Two of the stiffened plates cabinets cases which are quite widespread among various cabinets, are discussed next to illustrate the accuracy of this approach.

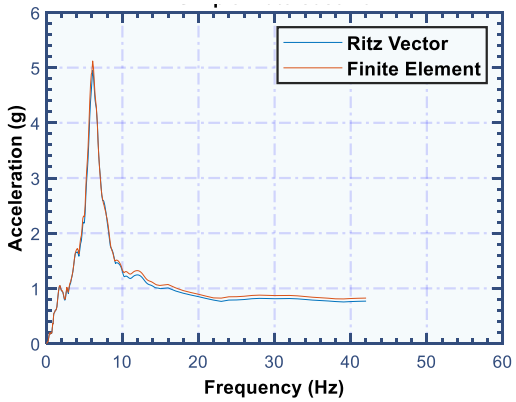

Figure 2. Comparison of In-cabinet response spectra between Ritz vector approach and Finite element analysis in *SAP2000*

Stiffened Plate Type 1

A stiffener restrains the free bending deformation of the plate where it is attached to the plate. If the stiffener has low stiffness, it bends as the plate bends, but if its stiffness is large compared to the bending stiffness of the plate, then it will apply a constraint in the bending of the plate. One such example of a stiffened plate is shown in Figure 3. The direction of the stiffener aligns with the minor axis of the plate, which prevents the free bending deformation of the plate in the *y* direction near the stiffener. The bending of the plate in the *x* direction remains unaffected and does not require additional Ritz vectors in this direction. The restrain in the bending of the plate in *y* direction can be reflected by superimposing additional Ritz vectors with a clamped boundary condition at both the ends as shown in Eq. (8).

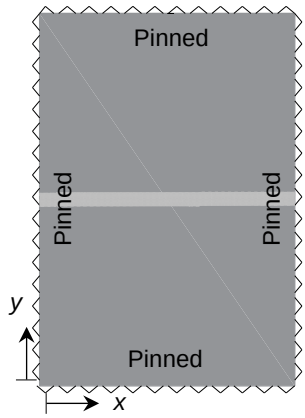

Figure 3. (a) Stiffened plate geometry with an intermediate horizontal stiffener

The deformation contour of the stiffened plate obtained from Ritz vector approach shows the double bending of the plate (Figure 4(a)). The side view deformation of the plate also reflects the same. The plot shown in Figure 4(b) compares the ICRS obtained from finite element analysis and the Ritz vector

approach. The plot shows that Ritz vector approach gives accurate ICRS as compared to that obtained by finite element analysis. Such complex double bending deformation of the stiffened plate is easily simulated through the Ritz vector approach simply by the addition of a few Ritz vectors.

$$\begin{aligned}\phi_{l1}(x,y) &= \psi_{ppx}(x)\psi_{ppy}(y)\\ \phi_{l2}(x,y) &= \psi_{ppx}(x)\psi_{pcy}(y)\\ \phi_{l3}(x,y) &= \psi_{ppx}(x)\psi_{cpy}(y)\\ \phi_{l4}(x,y) &= \psi_{ppx}(x)\psi_{ccy}(y)\end{aligned} \qquad \text{Eq. (8)}$$

where $\psi_{pp}(x)$ represents pinned-pinned boundary condition in the *x* direction; and $\psi_{ppy}(y)$ represents pinned-pinned, $\psi_{pcy}(y)$ represents pinned-clamped, $\psi_{pcy}(y)$ represents clamped-pinned and $\psi_{ccy}(y)$ represents clamped-clamped boundary condition in the *y* direction

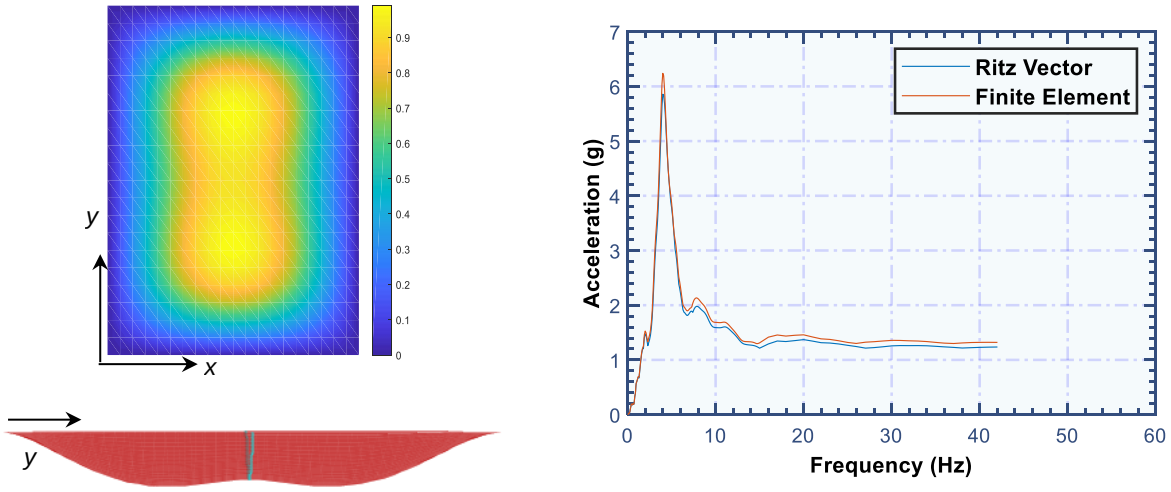

(a) (b)

Figure 4. Ritz vector approach for the stiffened plate: (a) Deformation contour and the shape of the plate & (b) Comparison of In-cabinet response spectra

Stiffened Plate Type 2

A stiffener generally has high torsional resistance if it has a closed cross-section whereas an open section stiffener has negligible torsional resistance. The torsional resistance of the stiffener influences the rotation of the plate at the location of its mounting. The stiffened plate in this case has a stiffener with high torsional resistance attached along an edge as shown in Figure 5(a). The stiffener in this plate would restrain the plate's rotation and would not allow the plate to rotate freely as a pinned boundary condition. This is a complex boundary condition because the stiffener is likely to constrain the rotation only partially in most cases, i.e. a stiffener with a very high torsional stiffness will be similar to a clamped condition with no rotation whereas a stiffener with a relatively lower value of torsional stiffness will create a boundary condition that constrains the rotation only partially.

The rotational constraint at the left edge of the plate can be incorporated by superimposing one additional Ritz vector representing clamped boundary condition as given in Eq. 9 and considering the

torsional stiffness of the stiffener. Figure 5(b) shows the deformation shape of the stiffened plate obtained by Ritz vector approach which also shows the restraint in rotation observed at the left edge. While analyzing this plate geometry with Ritz vector approach is straight forward, it is observed that the results do not compare well with the corresponding finite element analysis.

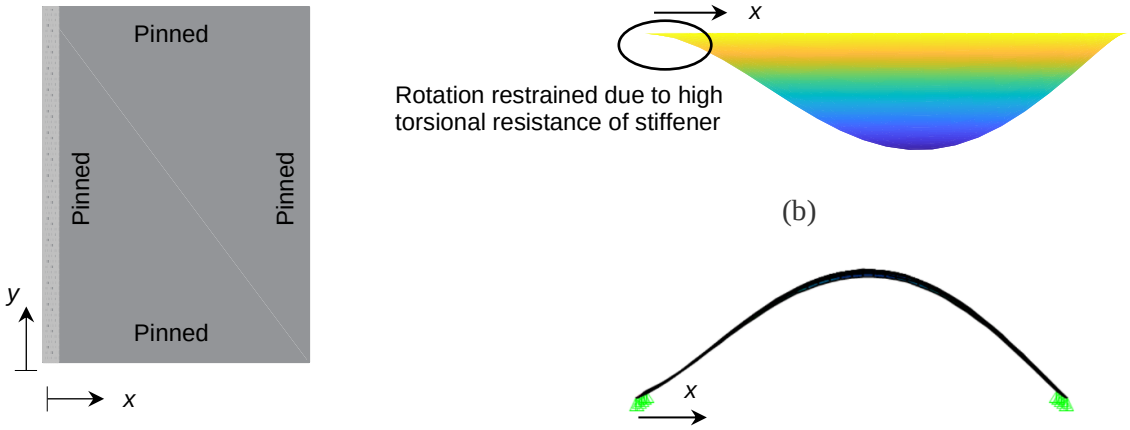

Figure 5. Stiffened plate geomtery and deformation shapes: (a) Stiffened plate geomtery, (b) Deformation shape obtained from Ritz vector approach & (c) Deformation shape by finite element analysis

Figure 5(c) shows the deformation shape of the same plate in the *x* direction obtained from a finite element analysis. As seen in this figure, the torsional resistance of the stiffener has almost no effect on the plate rotation at the left edge of the plate. The stiffener is modelled as line element in the finite element analysis and therefore does not offer any meaningful torsional resistance to the rotation of the plate. The stiffener must be modelled as 3D solid element in order to reflect the true behavior of the plate. Such consideration of torsional stiffness is often neglected in a finite element analysis which in turn leads to incorrect results in a finite element analysis. The various terms in the equation below are defined earlier in accordance with Eq. (8).

$$\phi_{l1}(x,y) = \psi_{pp}(x)\psi_{pp}(y)$$
$$\phi_{l2}(x,y) = \psi_{cp}(x)\psi_{pp}(y) \qquad \text{Eq. (9)}$$

SUMMARY AND CONCLUSIONS

This paper highlights the use of Ritz vector approach and illustrates its application to complex boundary conditions exhibited in the electrical cabinets and control panels. The approach is an efficient and accurate solution for developing the in-cabinet response spectra. The energy-based Ritz vector approach is mathematically rigorous and provides extremely accurate results. Identification of Ritz vectors with the help of engineering judgement and visualization of the deformation modes improved visualization of the complex deformations encountered in such systems. It is also illustrated that sometimes finite element analysis can lead to incorrect modelling assumption leading to inaccurate results whereas the Ritz vector approach works effectively even in such cases.

REFERENCES

[1] C. Rajalingham, R. B. Bhat and G. D. Xistris (1996), "Vibration of Rectangular Plates using Plate Characteristic Functions as Shape Functions in the Rayleigh-Ritz Method", *Journal of Sound and Vibration*, Vol. 193(2), pp. 497-509.

[2] C. S. Kim, P. G. Young and S. M. Dickinson (1990), "On the Flexural Vibration of Rectangular Plates Approached by using Simple Polynomials in the Rayleigh-Ritz method", *Journal of Sound and Vibration*, Vol. 143(3), pp. 379-394.

[3] G. N. Geannakakes (1995), "Natural Frequencies of Arbitrarily Shaped Plates using the Rayleigh-Ritz Method together with Natural Co-ordinate Regions and Normalized Characteristic Orthogonal Polynomials", *Journal of Sound and Vibration*, Vol. 182(3), pp. 441-478.

[4] Gupta, A., Rustogi, S. K. and Gupta, A. K. (1999a), "Ritz Vector Approach for Evaluation Incabinet Response Spectra", *Nuclear Engineering and Design*, Vol. 190, pp. 255-272

[5] Gupta, A., and Yang, J. F. (2002), "Modified Ritz vector approach for dynamic properties of electrical cabinets and control panels." *Nuclear Engineering and Design*, 217(1-2), 49–62.

[6] R. D. Blevins (1979), Formulas for Natural Frequency and Mode Shape, Van Nostrand Reinhold Company, New York.

[7] Rustogi, S. K., Gupta, A. and Gupta, A. K. (1998a), "Incabinet Response Spectra" *Technical Report C-NPP-SEP 21/98*, Dept. of Civil Engineering, North Carolina State University, Raleigh, NC.

[8] W. C. Hurty and M.F. Rubinstein (1964), Dynamics of Structures, Prentice-Hall, Inc. New Jersey.

[9] Yang, J., and Gupta, A. (2002), "Ritz vector approach for static and dynamic analysis of plates with edge beams." *Journal of Sound and Vibration*, 253(2), 373–388.

[10] Yang, J. F., Rustogi, S. K., and Gupta, A. (2003), "Rocking stiffness of mounting arrangements in electrical cabinets and control panels." *Nuclear Engineering and Design*, 219(2), 127–141.

[11] Z. Ding (1995), "Natural Frequencies of Elastically Restrained Rectangular Plates using a Set of Static Beam Functions in the Rayleigh-Ritz Method", *Computers & Structures*, Vol. 57, pp. 731-735.